

# Observation of the main phase transition of dinervonoylphosphocholine giant liposomes by fluorescence microscopy

Antti J. Metso<sup>a,b</sup>, Hongxia Zhao<sup>a</sup>, Ilkka Tuunainen<sup>a</sup>, Paavo K.J. Kinnunen<sup>a,c,\*</sup>

<sup>a</sup>*Helsinki Biophysics and Biomembrane Group, Institute of Biomedicine, University of Helsinki, Finland*

<sup>b</sup>*Department of Neurology, Helsinki University Central Hospital, Finland*

<sup>c</sup>*MEMPHYS-Center for Biomembrane Physics, University of Southern Denmark, Odense, Denmark*

Received 29 October 2004; received in revised form 22 April 2005; accepted 22 April 2005

Available online 13 June 2005

## Abstract

The phase heterogeneity of giant unilamellar dinervonoylphosphocholine (DNPC) vesicles in the course of the main phase transition was investigated by confocal fluorescence microscopy observing the fluorescence from the membrane incorporated lipid analog, 1-palmitoyl-2-(*N*-4-nitrobenz-2-oxa-1,3-diazol)aminocaproyl-*sn*-glycero-3-phosphocholine (NBDPC). These data were supplemented by differential scanning calorimetry (DSC) of DNPC large unilamellar vesicles (LUV, diameter  $\sim 0.1$  and  $0.2 \mu\text{m}$ ) and multilamellar vesicles (MLV). The present data collected upon cooling reveal a lack of micron-scale gel and fluid phase coexistence in DNPC GUVs above the temperature of  $20.5^\circ\text{C}$ , this temperature corresponding closely to the heat capacity maxima ( $T_{\text{em}}$ ) of DNPC MLVs and LUVs ( $T_{\text{em}} \approx 21^\circ\text{C}$ ), measured upon DSC cooling scans. This is in keeping with the model for phospholipid main transition inferred from our previous fluorescence spectroscopy data for DMPC, DPPC, and DNPC LUVs. More specifically, the current experiments provide further support for the phospholipid main transition involving a first-order process, with the characteristic two-phase coexistence converting into an intermediate phase in the proximity of  $T_{\text{em}}$ . This at least macroscopically homogenous intermediate phase would then transform into the liquid crystalline state by a second-order process, with further increase in acyl chain *trans*→*gauche* isomerization.

© 2005 Elsevier B.V. All rights reserved.

**Keywords:** Giant liposome; Phase transition

## 1. Introduction

Lipids provide the basic structural framework of all cellular membranes and, characteristically for liquid crystalline materials, exhibit a variety of different phases with connecting transitions [1]. The physical properties and thermodynamic state of the bilayer modulate both the activity and the lateral organization of the contained membrane proteins [2–4], while the proteins also determine in part the ordering of the lipids in the bilayer [5–7]. The molecular mechanisms underlying this dynamic interplay are being intensively investigated (e.g. [8–10]), as lateral heterogeneity and domain formation are known to be involved in several biological processes [11,12]. Biomembranes of eukaryote cells mainly exist in the fluid, liquid disordered state in physiological conditions. Yet, physical changes in the nerve membrane accompanying the prop-

**Abbreviations:**  $C_p$ , excess heat capacity; DMPC, 1,2-dimyristoyl-*sn*-glycero-3-phosphocholine; DNPC, 1,2-dinervonoyl-*sn*-glycero-3-phosphocholine; DPPC, 1,2-dipalmitoyl-*sn*-glycero-3-phosphocholine; GUV, giant unilamellar vesicle;  $\Delta H$ , enthalpy change; LUV, large unilamellar vesicle; MLV, multilamellar vesicle; NBDPC, 1-palmitoyl-2-(*N*-4-nitrobenz-2-oxa-1,3-diazol)aminocaproyl-*sn*-glycero-3-phosphocholine; PE, phosphatidylethanolamine; PC, phosphatidylcholine; PPDPC, 1-palmitoyl-2[10-(pyren-1-yl)]decanoyl-*sn*-glycero-3-phosphocholine;  $T$ , temperature;  $T_{\text{em}}$ , heat capacity maximum;  $T_m$ , main phase transition temperature (corresponding to 50% of the transition enthalpy);  $X_{\text{lipid}}$ , mole fraction of the indicated lipid

\* Corresponding author. Helsinki Biophysics and Biomembrane Group, Institute of Biomedicine/Medical biochemistry, Biomedicum, Haartmaninkatu 8, P.O. Box 63, FIN-00014, University of Helsinki, Finland. Fax: +358 9 19125444.

E-mail address: [Paavo.Kinnunen@Helsinki.Fi](mailto:Paavo.Kinnunen@Helsinki.Fi) (P.K.J. Kinnunen).

agation of action potential clearly involve a transient liquid disordered–ordered phospholipid phase change [1,13]. The physical properties and co-operative modes underlying thermal phase behavior of phospholipids also contribute to the established nanoscale lateral heterogeneity [14].

The theory of structural phase transition dynamics of soft materials remains incomplete [15]. The phase diagrams of multicomponent lipid mixtures can be exceedingly complex since, in addition to the different phases possible for single component membranes, there can be solid–solid [16,17], solid–fluid [18], as well as fluid–fluid [19,20] immiscibility. In order to establish a detailed description of the properties (including lateral organization) of lipid mixtures, it is mandatory to understand the mechanism of phase transition in single component membranes.

Dynamic lateral heterogeneity due to coexisting fluctuating gel and liquid crystalline domains accompanies the main transition of phospholipids [21–24]. Upon  $T \rightarrow T_m$  the intensity of these fluctuations are enhanced causing the bending elasticity and both lateral (area) and transversal compressibilities to have their maxima at  $T_m$  [25–27]. The permeability maximum of bilayers and augmented activity of phospholipases  $A_2$  near  $T_{em}$  have been attributed to the length of the phase boundary also having a maximum at  $T_{em}$  [28–30]. Many of the previous studies on main phase transition have assumed the heat capacity maximum to be identical to  $T_m$  [25,26]. However, transition temperature  $T_m$  is, by definition, the melting point where 50% of the transition is completed and it is thus not necessarily identical to the temperature of the heat capacity maximum ( $T_{em}$ ), particularly in the case of strongly asymmetric  $C_p$  peaks [31,32].

Our previous studies on the main transition of phospholipid LUVs suggest that the discontinuities seen in the fluorescence properties may require modification of the existing models describing the phospholipid main transition as a first-order process involving only gel and fluid phases. More specifically, we have recently forwarded a more detailed description of the main transition based on time-resolved fluorescence spectroscopy of DPPC and DNPC [31,32]. In brief, characteristically to a first-order transition, fluid-like domains start to form in the gel phase bilayer upon heating. This fraction of the ‘melted’ lipids and the length of the interfacial boundary both increase with temperature, i.e. with the progression of the transition. In keeping with the model by Heimburg [33], the fluid-like domains would start to form in the line defects initiated at the corrugations appearing at  $T_p$ . Upon approaching  $T_{em}$ , the phase boundary seems to disappear, with the formation of an intermediate phase. The latter was suggested to result from the properties of the coexisting fluid-like and gel phases approaching each other as two parallel second-order processes developing with temperature, causing progressively diminishing line tension and hydrophobic mismatch. At  $T_{em}$ , fluctuations would be most intense, the entire membrane reaching an intermediate phase and becoming equivalent to the ‘boundary’-like lipids. This strongly fluctuating intermedi-

ate phase would then transform into the liquid disordered phase as a second-order transition with weak first-order characteristics due to heterophase fluctuations [34], with further increase in acyl chain *trans*→*gauche* isomerization. Upon the completion of this process, the bilayer is in a liquid disordered phase [32,35].

The above model was mainly derived from the behavior of a pyrene-labelled fluorescent phospholipids derivative 1-palmitoyl-2[10-(pyren-1-yl)]decanoyl-*sn*-glycero-3-phosphocholine (PPDPC) in DMPC [36], DPPC [31], and DNPC [32] matrices. Accordingly, it must be emphasized that because of the presence of the fluorophore, we were observing the transition of an ‘impure’ lipid matrix and the mechanism forwarded applies in strict sense to the bilayer melting in the presence of the contained probes.

In the current study, we addressed the putative intermediate phase by confocal microscopy of dinervonoylphosphocholine (DNPC) giant liposomes using NBD-labeled phosphocholine as the fluorescent probe ( $X=0.02$ ). DNPC contains very long 24:1-*cis*15 chains and thus forms significantly thicker bilayers than DPPC, for instance. We are not aware of DNPC being found in cells and its use as a model was merely dictated by the possibility of being able to study the macroscopic organization of a bilayer undergoing thermal phase transition using fluorescence microscopy. The augmented partitioning of NBD-labelled phosphatidylcholine analogs into the liquid disordered phase has been utilized to observe the coexisting micron-scale phases in the course of the main transition [37,38]. The impact of the fluorescent probe on the main phase transition of the matrix phospholipid was studied by differential scanning calorimetry (DSC).

## 2. Materials and methods

### 2.1. Materials

1,2-nervonoyl-*sn*-glycero-3-phosphocholine (DNPC) and 1-palmitoyl-2-(*N*-4-nitrobenz-2-oxa-1,3-diazol)aminocaproyl-*sn*-glycero-3-phosphocholine (NBDPC) were from Avanti Polar Lipids (Alabaster, USA). The concentration of DNPC was determined gravimetrically. In brief, 50  $\mu$ l aliquot of the lipid in chloroform was transferred with a Hamilton microsyringe onto weighing pans. The solvent was subsequently removed under a gentle flow of nitrogen and keeping the samples under reduced pressure for approx. 1 h before recording the weight of the lipid residue with a high-precision electrobalance (Cahn 2000, Cahn Inc., Cerritos, USA). The concentration of NBDPC was determined by spectroscopy using a molar absorptivity  $\epsilon_{465}=19,000$  (in  $C_2H_5OH$ ). The purity of the lipids was checked by thin layer chromatography on silic acid coated plates (Merck, Darmstadt, Germany) using chloroform/methanol/water (65/25/4, v/v/v) as eluent. An examination of the plates after iodine staining or upon UV-illumination

revealed no impurities. The buffer used in DSC experiments was 20 mM HEPES, 0.1 mM EDTA, pH 7.0, prepared in freshly deionized Milli RO/Milli Q water (Millipore, Bedford, USA) with the pH adjusted with NaOH. The buffer used in giant liposome experiments was 0.5 mM HEPES, pH 7.4.

## 2.2. Preparation of liposomes

Lipids were dissolved and mixed in chloroform to yield the indicated compositions, where after this solvent was removed under a stream of nitrogen. The lipid residue was subsequently maintained under reduced pressure for at least 4 h and then hydrated at 60 °C, i.e. above the main transition temperature  $T_m$  of DNPC (26 °C) to yield multilamellar vesicles at a lipid concentration of 0.7 mM. To obtain unilamellar vesicles the hydrated lipid mixtures were extruded with a LiposoFast small-volume homogenizer (Avestin, Ottawa, Canada) above  $T_m$ . Samples were subjected to 19 passes through one polycarbonate filter (0.1 or 0.2  $\mu\text{m}$  pore size, Nucleopore, Pleasanton, USA). Extrusion through filters with 100 nm and 200 nm pores typically yield LUVs with a mean diameter of  $130 \pm 10$  nm and  $170 \pm 15$ , respectively [39,40], and the fraction of vesicles with more than two bilayers should be less than 15% [40]. Minimal exposure of the lipids to light was ensured throughout the procedure. Subsequently, the liposome solutions were divided into proper aliquots and diluted with the above buffer for DSC.

## 2.3. Differential scanning calorimetry

Heating and cooling heat capacity scans were recorded using VP-DSC microcalorimeter (Microcal Inc., Northampton, USA) at a rate of either 5°/h or 30°/h, as indicated, and using final lipid concentration of 0.7 mM in the DSC cell. The obtained endotherms were analyzed using the routines of the software provided by the instrument manufacturer.

## 2.4. Confocal fluorescence microscopy of giant liposomes

Giant liposomes were prepared as described elsewhere [41]. Approx. 2 to 4  $\mu\text{l}$  of the indicated lipids dissolved in diethylether:methanol (9/1, v/v) at a concentration of 1 mM was applied onto the surface of two Pt electrodes and subsequently dried under a stream of nitrogen. Possible residues of the organic solvent were removed by evacuation for 1 h. A glass chamber with the attached electrodes and a quartz window bottom was placed on the stage of an inverted fluorescence microscope (Olympus IX 70, Olympus Optical Co., Tokyo, Japan). The temperature was maintained at 35 °C and an AC field (sinusoidal wave function with a frequency of 8 Hz and amplitude of 0.2 V) was applied before adding 1.5 ml of 0.5 mM HEPES buffer, pH 7.4. During the first minute of hydration, the voltage was

increased to 2 V. The AC field was turned off after 2 h and giant liposomes were observed with differential interference contrast (DIC) optics with a 20/0.40 objective. The temperature in the chamber was controlled with a thermoelectric module (TS-4, Physitemp Instruments, Inc., Clifton, USA) and monitored using a thermal probe (Type T thermocouple: IT-18, Physitemp Instruments, Inc., Clifton, USA) immersed in the chamber and connected to a thermometer (DP41, Omega Engineering, Inc., Stamford, USA). The sizes of GUVs were measured using calibration of the images by motions of the micropipette as proper multiples of the step length (50 nm) of the micromanipulator (MX831 with MC2000 controller, SD Instruments, Grants Pass, USA). The diameter of the DNPC vesicles formed varied between 10 and 50  $\mu\text{m}$ . Fluorescent images were obtained using the above inverted microscope with a confocal optical scanner (Yokogawa Inc., Tokyo, Japan) and an argon ion laser (Melles Griot 643R, Carlsbad, USA) with 488 nm excitation wavelength. Images were recorded with a Peltier-cooled 12-bit digital CCD camera C4742-95 (Hamamatsu Inc., Hamamatsu City, Japan), interfaced to a computer, and operated by the software (HiPic 5.0.1 or Aquacosmos 1.2) provided by the camera manufacturer.

## 3. Results

### 3.1. Differential scanning calorimetry

We have previously reported on the thermal phase behavior of DNPC MLVs and LUVs assessed by DSC heating scans [32]. As the preliminary experiments on the thermal behavior of DNPC GUVs showed only cooling scans to be feasible (see below), differential heat capacity scans for DNPC MLVs and LUVs were recorded upon heating and cooling by DSC. Since both the vesicle size as well as the included phospholipid analog could influence the phase behavior, we first studied neat MLVs and LUVs, the latter extruded using two different filter pore sizes, 0.1  $\mu\text{m}$  and 0.2  $\mu\text{m}$ . The enthalpy peak (with a maximum heat capacity at  $T_{em} \approx 26.8$  °C) for neat DNPC MLVs upon heating is asymmetric, with 47.4 kJ/mol below and 14.6 kJ/mol above  $T_{em}$ . The corresponding cooling scan exhibits a broad exotherm followed by a sharp major exotherm at 21.8 °C (Fig. 1), with a combined enthalpy of 64.6 kJ/mol (Table 1). Repeating the heating–cooling cycle reproduced the above features independent from the scan rate, varying between 5°/h and 10°/h (data not shown). For MLVs, the  $T_{em}$  reported corresponds to the temperature of the major enthalpy peak, while the values for  $\Delta H$  represent the underlying total enthalpies in the peaks. The origin of the high temperature shoulder upon cooling of MLVs is at present unclear. However, differences in the geometrical constraints and changes in the bilayer hydration between the thermal cycles could explain the observed inequality of the  $C_p$  peaks (see Discussion).

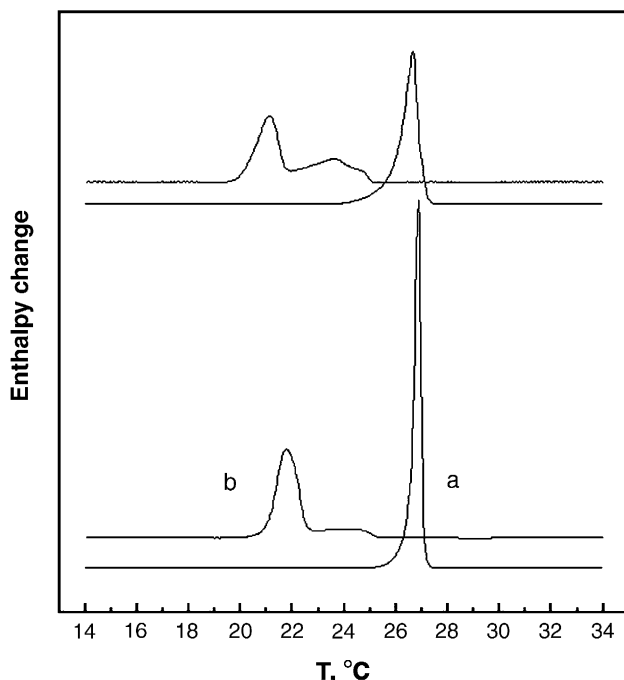


Fig. 1. Differential heat capacity traces upon the heating (a) and cooling (b) of DNPC MLVs. The upper traces were recorded for liposomes containing the fluorescent phospholipid analog NBDPC ( $X=0.02$ ). The total lipid concentration was 0.7 mM in 20 mM HEPES, 0.1 mM EDTA, pH 7.0.

The extrusion of MLVs to yield LUVs broadens the observed enthalpy peaks for both neat DNPC liposomes and those containing the fluorescent lipids. We have suggested this broadening to reflect reduced co-operativity and coherence of the membrane due to a lack of interbilayer coupling, with both the increased curvature of the vesicles and the smaller size of the LUVs limiting the maximum size of the co-operative unit [31]. In contrast to MLVs, repeated heating and cooling cycles for DNPC LUVs exhibited single endo- and exotherms, respectively, with approximately equal enthalpies (Fig. 2). Similarly to MLVs, the heat capacity scans for DNPC LUVs are characterized by a pronounced hysteresis of  $\sim 5^\circ$  with  $T_{em}$  at  $\sim 26$  and  $\sim 21^\circ\text{C}$  upon heating and cooling, respectively. The  $T_{em}$  for LUVs obtained by extrusion through a  $0.2\ \mu\text{m}$  pore size filter exceeded by  $0.3^\circ$  the  $T_{em}$  for LUVs extruded through  $0.1\ \mu\text{m}$  pores (Table 1). Because of the loss of lipid in the extrusion through the polycarbonate filter, reliable values for the transition enthalpies could not be obtained for LUVs. No significant change in the width of the enthalpy peak was observed for these LUVs. Instead, the effect of the number of layers (MLV vs. LUV) on the width of the enthalpy peak was pronounced (Figs. 1 and 2), and compared to LUV cooling scans, the heating scans for LUVs show a broader enthalpy peak, yet remain asymmetric (Fig. 2).

The fluorescent phospholipid analog NBDPC used in this study represents a substitutional impurity in the DNPC matrix and should thus broaden the endotherms. Previous studies on main transition have shown that fluorescent

Table 1

Values for  $T_{em}$  (in  $^\circ\text{C}$ ) and enthalpy (kJ/mol) measured by DSC for MLV and LUV cooling scans of different lipid compositions (in mole fractions, within brackets)

Vesicle composition	$T_{em}$	$\Delta H$
<i>MLV</i>		
DNPC (1.00)	21.8	64.6
DNPC/NBDPC (0.98/0.02)	21.0	66.3
<i>LUV</i>		
DNPC (1.00)	21.0	n.a.
DNPC/NBDPC (0.98/0.02) pore size $0.1\ \mu\text{m}$	20.7	n.a.
DNPC/NBDPC (0.98/0.02) pore size $0.2\ \mu\text{m}$	21.0	n.a.

The total lipid concentration in the DSC cell was 0.7 mM for MLVs, whereas because of the loss of lipid in the extrusion through the polycarbonate filter, reliable values for the transition enthalpies could not be measured for LUVs. The buffer was 20 mM HEPES, 0.1 mM EDTA, pH 7.0.

probes may also modestly decrease the temperature of the heat capacity maximum [31,36]. This effect was observed also in the present study. Accordingly, the presence of NBDPC ( $X_{\text{NBDPC}}=0.02$ ) in DNPC MLVs lowers  $T_{em}$  from 21.8 to  $21.0^\circ\text{C}$ , with slight broadening of the peak (Table 1). The freezing point depression effect by the fluorescent probes could result from their preferential partitioning into the interfacial boundary between coexisting the fluid and gel state domains in the transition region [25–27], as reported earlier for PPDPC in DMPC [36] and DPPC [31]. This enrichment would stabilize the boundary and thus favor the formation of the nascent phase at lower temperatures.

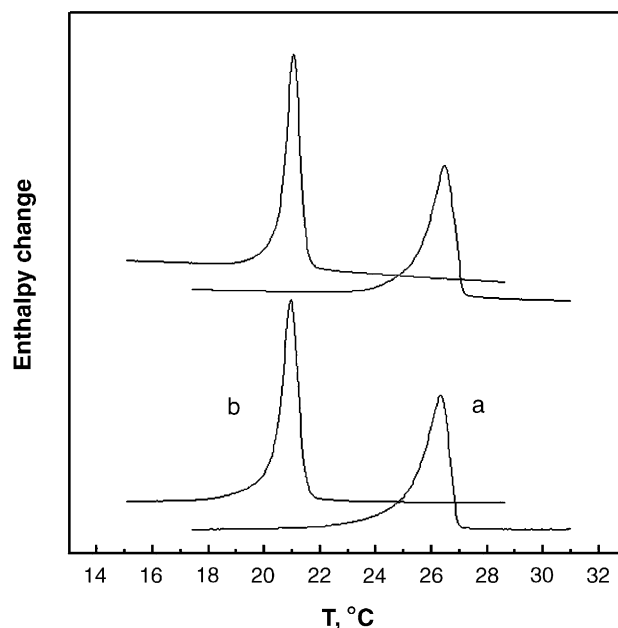


Fig. 2. Differential heat capacity traces upon the heating (a) and cooling (b) of DNPC LUVs obtained by extrusion through  $0.2\ \mu\text{m}$  pores. The upper traces were recorded for the liposomes containing the fluorescent phospholipid analog NBDPC ( $X=0.02$ ). The buffer was 20 mM HEPES, 0.1 mM EDTA, pH 7.0.



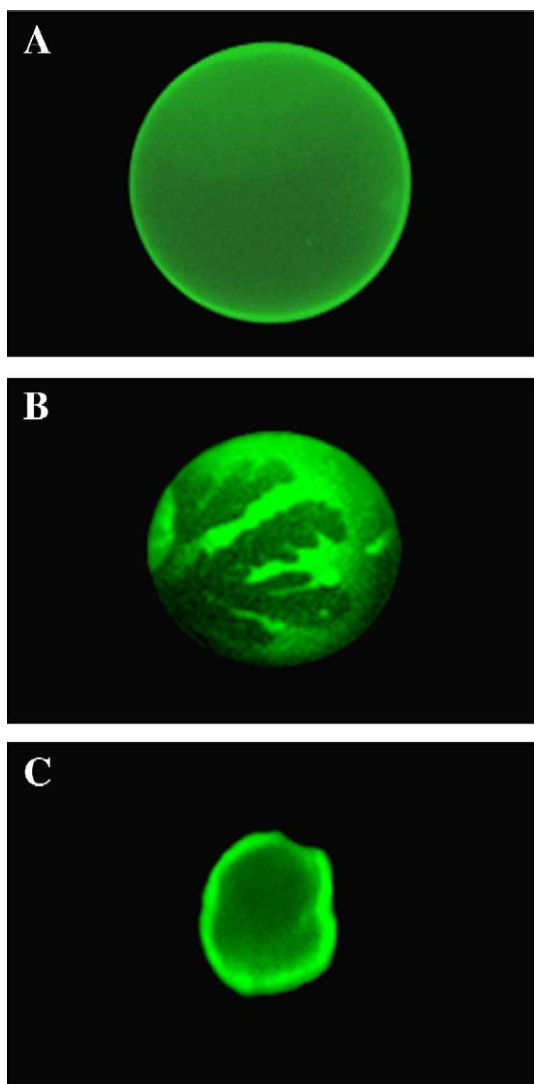


Fig. 3. Confocal microscopy images for DNPC/NBDPC (0.98/0.02) GUV observed upon cooling, with  $T_{em}=21$  °C, defined as the heat capacity maximum measured from the exotherm of the corresponding LUVs (extruded through 0.2  $\mu\text{m}$  filters). Panel A:  $(T - T_{em})=4$  °C; Panel B:  $(T - T_{em})=-0.5$  °C; Panel C:  $(T - T_{em})=-1.5$  °C.

### 3.2. Confocal microscopy

The phase transition of DNPC giant vesicles containing the fluorescent phospholipids analog NBDPC ( $X_{\text{NBDPC}}=0.02$ ) was studied during cooling scans between  $6 > (T - T_{em}) > -3$  °C, with  $T_{em}$  derived from the cooling scans for DNPC LUVs ( $\varnothing \approx 0.2$   $\mu\text{m}$ ). It is possible that the actual thermal phase transition of equivalent GUVs is broader and the  $T_{em}$  slightly higher than that measured for LUVs, as suggested by the DSC data for different sized LUVs. Accordingly, Brumm and coworkers [42] reported that for cooling scans of supported binary bilayers, the highest  $T_{em}$  value was measured for planar membranes, while the lowest value was found for small unilamellar vesicles (SUVs). These authors concluded that an increase in membrane curvature lowers the equilibrium lateral pressure of the lipid membrane, which causes

the temperature shift. The predicted broadening of the phase transition of GUVs with respect to that found in MLVs is, in part, also explained by the intrinsic difference between the structures of the GUVs and MLVs, the latter representing a stack of bilayers. Related to this, it appears that the thermal phase behavior of LUVs rather than MLVs corresponds more closely to the thermal behavior of GUVs.

Based on the fluorescence spectroscopy and DSC data, we have previously suggested the presence of an intermediate phase in the course of main phase transition [31]. Accordingly, the absence of micron-scale gel and fluid phase coexistence above  $T_{em}$  was proposed, with heterophase fluctuations in the nanometer scale [32,35]. The present data show that upon reducing temperature from  $(T - T_{em}) \approx 7$  to 1 °C, the vesicle sizes remain almost unchanged (Fig. 3). When  $(T - T_{em}) \approx 1$  °C is reached, the GUVs start to shrink. Importantly, lateral distribution of the NBDPC probe in DNPC GUVs remains homogenous until  $(T - T_{em}) \approx -0.5$  °C (i.e. 20.5 °C). At this temperature, dark domains become visible while the GUVs continue to shrink. The gradual decrease in the vesicle diameter was approximately 25% for vesicles with diameters in the range 15 to 25  $\mu\text{m}$ , whereas changes of  $\sim 15\%$  were observed for the smallest GUVs (diameters ranging from 5 to 15  $\mu\text{m}$ , Fig. 4). Related to this, a decrease in vesicle diameters by approx. 7–8% in the course of the main transition has been reported for DMPC and DPPC GUVs [43,44]. Importantly, in these experiments, no concomitant rupture of the vesicles was observed. After approx. 2 min at  $(T - T_{em}) \approx -0.5$  °C, the

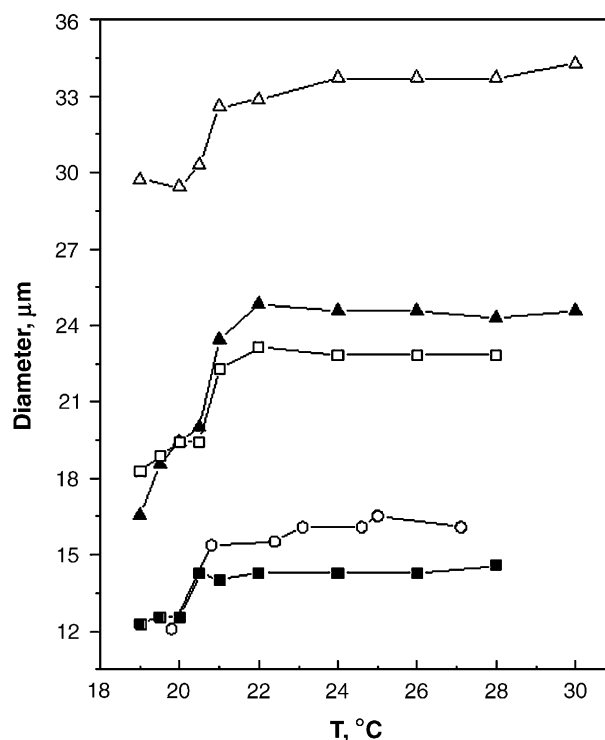


Fig. 4. Change of diameter ( $\mu\text{m}$ ) of five DNPC/NBDPC (0.98/0.02) GUVs as a function of temperature during cooling.

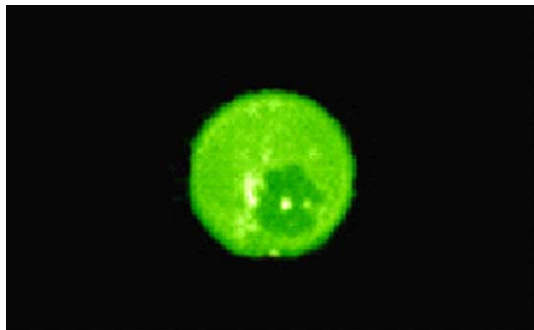


Fig. 5. Confocal microscopy image for DNPC/NBDPC (0.98/0.02) GUV observed upon cooling at  $(T - T_{em}) = -0.5$  °C, with  $T_{em} = 21$  °C, defined as the heat capacity maximum measured from the exotherm of the corresponding LUVs (extruded through 0.2  $\mu$ m filters).

fluorescent probes in most vesicles cluster along the edges of the black domains (Fig. 5). As the temperature is decreased further to  $(T - T_{em}) \approx -1$  °C, the relative size of the dark domains in the intact vesicles increases. Simultaneously with the appearance of the dark domains, i.e. the coexistence of gel and fluid phases at  $(T - T_{em}) \approx -0.5$  °C, vesicles have a tendency to detach from the Pt-wire. After reaching  $(T - T_{em}) \approx -1.5$  °C, most of the GUVs had detached from the electrode and collapsed, ending up as small particles (Fig. 3, panel C). This process did depend on the size of the giant liposomes so that the decrease in the diameter of the largest vesicles occurred at higher temperatures. Interestingly, most vesicles collapsed in the gel–fluid coexistence region, before reaching the gel phase. Upon heating of the intact vesicles, the diameters increased almost linearly and the giant liposomes became homogenous at  $T \approx 26$  °C, this temperature coinciding with the  $T_{em}$  value measured by DSC for the heating scan of the corresponding LUVs. However, only modest recovery of the GUV diameter ( $\sim 73\%$ ) was observed, suggesting lipid loss during the cooling scan. No shape hysteresis was observed, in contrast to the study by Bagatolli and Gratton [43] reporting shape hysteresis and lack of temperature hysteresis for the main transition of DPPC and DMPC GUVs.

#### 4. Discussion

Our previous studies on main transition have indicated the lack of a true two phase region for DMPC and DPPC at temperatures  $T > T_{em}$  [31,36]. Accordingly, we have suggested the transition to proceed upon heating initially as a first order process with coexisting solid ordered and liquid disordered phase (up to approx.  $T_{em}$ ) and, subsequently, as a second order process, in which a putative intermediate phase converts into the true liquid disordered phase [31,32,35,36]. This model was assessed in the present study by observing giant vesicles composed of DNPC by fluorescence imaging. More specifically, we studied DNPC giant vesicles undergoing main phase transition by confocal microscopy and

using NBD-labeled fluorescent phospholipid partitioning preferentially into the fluid, liquid disordered phase [35]. This probe has a strong tendency for self-quenching [45], and in monolayers of pure NBD-labeled lipids, there is evidence for hydrogen bond mediated interactions between the NBD moieties [46]. Aggregation and self-quenching of NBD-lipids in the gel phase is supported by analysis of the fluorescence lifetimes for a headgroup-labeled NBD-phospholipid analog [47]. In the fluid phase and for NBD attached to the acyl chain, the fluorescent NBD moiety is partly distributed into the interface [48,49].

Intriguingly, our microscopy data reveals a lack of micron-scale coexistence of gel and fluid phases at temperatures above the  $T_{em}$  of DNPC LUVs. Yet, it must be emphasized that the absence of the two-phase region at  $T > T_{em}$  could be apparent only and be due to the limited resolution of the microscope. Accordingly, the possibility of nanometer-scale gel/fluid coexistence at these temperatures [43] cannot be explicitly excluded. However, our data do not support two-state transition models that assume ‘large-scale’ gel/fluid coexistence above the heat capacity maximum [50], and align instead with the interpretation of our previous results obtained with fluorescent probes [31,32,36]. Importantly, our model does readily comply with the so-called anomalous swelling seen for saturated PCs [51,52]. More specifically, the sharp, non-linear increase in the interbilayer repeat distance observed by X-ray scattering has been suggested to be caused by softening of the bilayers causing entropic repulsion between the bilayers. Intriguingly, the anomalous swelling coincides with the region which our model postulates to be the strongly fluctuating intermediate phase.

DSC measurements cannot be accomplished for giant vesicles, and the thermal phase behavior of DNPC GUVs as well as the impact of the fluorescent probe, NBD-PC, had to be deduced from the DSC data of DNPC LUVs. Although the actual difference is likely to be small, LUVs seem to exhibit narrower endo- and exotherms and perhaps also somewhat lower values for  $T_{em}$  than GUVs [42,43]. Fourier transform infrared spectroscopy and DSC data for DMPC and DSPC (1:1) membranes on a solid support with varying curvatures suggest that with increasing curvature, the temperatures of the liquidus and solidus points are shifted to lower values by up to 7° and 15°, and the mixing of the two lipid species in the two-phase region is altered [42]. It was further shown that planar membranes have the highest transition temperatures, while the lowest value is found for small unilamellar vesicles. Theoretical considerations suggest that the shift of the liquidus point can be understood as a reduction in the equilibrium lateral pressure of the bilayer with an increasing vesicle curvature [42]. In keeping with the latter study, our present data on LUVs reveals that the  $T_{em}$  for LUVs obtained by extrusion through a 0.2  $\mu$ m pore size filter exceeded by 0.3° the  $T_{em}$  for LUVs extruded through 0.1  $\mu$ m pores (Table 1). Instead, the curvature

appears to have a smaller impact on the width of the enthalpy change.

A pronounced hysteresis of about 5° for the strongly asymmetric enthalpy peaks is observed for both DNPC MLVs and LUVs. There is no reason to expect this to apply also to GUVs. The molecular level processes associated with the thermal hysteresis of phospholipid phase changes are incompletely understood. However, the increased repulsion between the acyl chains because of increasing acyl chain lengths or chain unsaturation appears to play an important role in the width of the hysteresis [53]. This polymorphism is likely to enhance the expansive impact of *trans* ↔ *gauche* isomerization in the course of the main transition resulting in metastable intermediates and the observed hysteresis upon cooling [54]. The enthalpy change associated to the phenomenon of hysteresis not necessarily has to be symmetric, and the asymmetric enthalpy peaks of DNPC observed here could reflect the sum of multi-component transitions, as reported for PE dispersions [55,56]. Yet, unlike for PCs, direct intermolecular hydrogen bonding at the headgroup level is possible for PE, which could make the molecular mechanisms associated with the melting of bilayers comprised of this lipid more complex.

Notably, according to our interpretation of the data for DMPC, DPPC, and DNPC, the transition would be a multicomponent process, progressing upon heating first as first-order process with true gel–fluid co-existence region until  $T_{em}$ , where after these, phases merge due to intense fluctuations into an intermediate phase, developing into true fluid phase by a second-order process. Unlike PEs that do not display a pretransition, PCs exhibit a low co-operativity pretransition that merges with the main transition [33]. The broadening of the low temperature region of the DNPC MLV and LUV enthalpy peaks could correspond to pretransitional reorganization, and the formation of periodic membrane ripples, occurring at these temperatures. More specifically, the ripples are considered to be one-dimensional defects of fluid lipid molecules that cause a local bending of the membrane [33]. The number of fluid lipid line defects would be approximately equal in both monolayers to minimize the free energy superimposed by geometrical boundary conditions. Yet, the number of bilayers is likely to influence the domain growth, as discussed below.

The existence of a highly cooperative sub-main transition has been reported for multilamellar bilayers composed of long-chain saturated diacyl phosphatidylcholines [57–59]. This transition takes place over a narrow temperature range positioned between the pretransition and main transition. The associated enthalpy change is a few percent of the transition enthalpy for the corresponding main transition [58]. Since the pretransition of the unsaturated DNPC vesicles merges with the main transition, we cannot exclude the possibility that a similar transition would occur also for DNPC. However, a sub-main transition would appear as a relatively narrow

anomaly in the DSC trace. The absence of such change for DNPC suggests that the decoupling of the translational and conformational variables, other than pretransition, would not contribute to the observed endotherm.

Although not being the main focus of the present study, it is worth mentioning that the splitting of the DSC curve for the MLV cooling scan (Fig. 1) is enigmatic. The thermal behavior of MLVs upon cooling should be basically similar to that of GUVs. Rather than a two-state process, Rappolt and Rapp [56] have suggested the main transition to be a sequence of transitions, with different cluster growth modes from the gel to the liquid crystalline phase and vice versa. The main difference between the thermal cycles is the area per lipid molecule of the initial phase that is significantly greater for the fluid bilayer. In order to keep the system at its energy minimum, the transition would start at the outer shells of the liposomes upon heating, and inner shells upon cooling. The broad component of the MLV cooling scan is thus likely to reflect crystallization of the inner bilayers of the liposome. This second-order transition first proceeds in both radial and tangential directions. The corresponding increase in the interfacial tension is modest, and no extensive interface boundaries within the emerging intermediate phase are observed, in keeping with diffusion controlled kinetics. Weak geometrical constraints and steric hindrance occurring between the inner and outer bilayer shells and between the fluid and intermediate phase regions presumably contribute to the observed thermal phase behavior of the MLVs. As demonstrated by Rappolt and Rapp, these curvature-induced constraints are expected to be less perturbing upon heating [56].

In the context of the present data, it is important to consider the possibility of slow formation of the nascent phase in the course of the transition. Slow rearrangement modes with relaxation times exceeding the experimental time scales could influence the observed thermal phase behaviour of the liposomes. Related to this, X-ray diffraction and temperature oscillation calorimetry measurements demonstrate that the main transition for DPPC MLVs is fast (transit times of less than 1 s) on heating and very slow on cooling extending to time scale of hours [60,61]. These data, collected with slow heating rate (0.05–0.5 °C/min), reveal a loss of long-range order in the interbilayer lattice in a narrow temperature range of ~100 mK. In contrast, data measured by IR-laser induced rapid T-jump techniques display a well-concentrated transition without loss of order [62]. Under the conditions of the latter experiment, the transition is clearly discontinuous between the two states with a half-life for the development of the product phase signal of about 10 ms. These data suggest that a difference in the driving force and the rate of the thermal cycle may lead to differences in the transition order. However, our present static excess  $C_p$  data with a heating/cooling rate varying between 5°/h and 30°/h exhibit the same irreversible characteristics, independent of the scan rate.

## Acknowledgements

The authors wish to thank Dr. Arimatti Jutila for rewarding discussions and the anonymous reviewer for bringing the anomalous swelling to our attention. Technical assistance by Kaija Niva and Kristiina Söderholm is appreciated. A.J.M. acknowledges grants from the Research and Science Foundation of Famos and Suomen Lääketehteen Säätiö. HBBG is supported by the Finnish Academy and Sigrid Juselius Foundation and Memphys by The Danish National Research Foundation.

## References

- [1] P.K.J. Kinnunen, P. Laggner (Eds.), *Chem. Phys. Lipids* 57 (2–3) (1991) 109–408 (Special Issue).
- [2] P. Mustonen, J.A. Virtanen, P.J. Somerharju, P.K.J. Kinnunen, Binding of cytochrome *c* to liposomes as revealed by the quenching of fluorescence from pyrene-labeled phospholipids, *Biochemistry* 26 (1987) 2991–2997.
- [3] T. Hønger, K. Jørgensen, D. Stokes, R.L. Biltonen, O.G. Mouritsen, Phospholipase A<sub>2</sub> activity and physical properties of lipid–bilayer substrates, *Methods Enzymol.* 286 (1997) 168–190.
- [4] W.L.C. Vaz, P.F.F. Almeida, Phase topology and percolation in multiphase lipid bilayers: is the biological membrane a domain mosaic? *Curr. Opin. Struct. Biol.* 3 (1993) 482–488.
- [5] O.G. Mouritsen, M. Bloom, Mattress model of lipid–protein interactions in membranes, *Biophys. J.* 46 (1984) 141–153.
- [6] F.J. Asturias, D. Pascolini, J.K. Blasie, Evidence that lipid lateral phase separation induces functionally significant structural changes in the Ca<sup>2+</sup>-ATPase of the sarco-plasmic reticulum, *Biophys. J.* 58 (1990) 205–217.
- [7] J.Y.A. Lehtonen, P.K.J. Kinnunen, Evidence for phospholipid microdomain formation in liquid crystalline liposomes reconstituted with *Escherichia coli* lactose permease, *Biophys. J.* 72 (1997) 1247–1257.
- [8] O.G. Mouritsen, P.K.J. Kinnunen, Role of lipid organization and dynamics for membrane functionality, in: K.M. Merz, B. Roux (Eds.), *Biological Membranes*, Birkhäuser, Boston, 1996, pp. 463–502.
- [9] O.G. Mouritsen, Self-assembly and organization of lipid–protein membranes, *Curr. Opin. Colloid Interface Sci.* 3 (1998) 78–87.
- [10] J.M. Holopainen, A.J. Metso, J.-P. Mattila, A. Jutila, P.K.J. Kinnunen, Evidence for the lack of a specific interaction between cholesterol and sphingomyelin, *Biophys. J.* 86 (2004) 1510–1520.
- [11] P.K.J. Kinnunen, On the principles of functional ordering in biological membranes, *Chem. Phys. Lipids* 57 (1991) 375–399.
- [12] R. Welti, M. Glaser, Lipid domains in model and biological membranes, *Chem. Phys. Lipids* 73 (1994) 121–137.
- [13] P.K.J. Kinnunen, J.A. Virtanen, A qualitative, molecular model of the nerve impulse: conductive properties of unsaturated lyotropic liquid crystals, in: F. Gutmann, H. Keyzer (Eds.), *Modern Bioelectrochemistry*, Plenum Press, NY, 1986, pp. 457–479 (Chapt. 17).
- [14] F. Dumas, M.C. Lebrun, J.F. Tocanne, Is the protein/lipid hydrophobic matching principle relevant to membrane organization and functions? *FEBS Lett.* 458 (1999) 271–277.
- [15] P. Laggner, M. Krichbaum, Phospholipid phase transitions: kinetics and structural mechanisms, *Chem. Phys. Lipids* 57 (1991) 121–145.
- [16] B.R. Lentz, B.J. Litman, Effect of head group on phospholipid mixing in small, unilamellar vesicles: mixtures of dimyristoylphosphatidylcholine and dimyristoylphosphatidylethanolamine, *Biochemistry* 17 (1978) 5537–5543.
- [17] S.H. Untracht, G.G. Shipley, Molecular interactions between lecithin and sphingomyelin. Temperature- and composition-dependent phase separation, *J. Biol. Chem.* 252 (1977) 4449–4457.
- [18] R.E. Pagano, R.J. Cherry, D. Chapman, Phase transitions and heterogeneity in lipid bilayers, *Science* 181 (1973) 557–559.
- [19] D.J. Recktenwald, H.M. McConnell, Phase equilibria in binary mixtures of phosphatidylcholine and cholesterol, *Biochemistry* 20 (1981) 4505–4510.
- [20] S.H.W. Wu, H.M. McConnell, Phase separations in phospholipid membranes, *Biochemistry* 14 (1975) 847–854.
- [21] D. Marsh, A. Watts, P.F. Knowles, Cooperativity of the phase transition in single- and multibilayer lipid vesicles, *Biochim. Biophys. Acta* 465 (1977) 500–514.
- [22] S. Doniach, Thermodynamic fluctuations in phospholipid bilayers, *J. Chem. Phys.* 68 (1978) 4912–4916.
- [23] E. Freire, R. Biltonen, Estimation of molecular averages and equilibrium fluctuations in lipid bilayer systems from the excess heat capacity function, *Biochim. Biophys. Acta* 514 (1978) 54–68.
- [24] O.G. Mouritsen, K. Jørgensen, T. Hønger, Permeability of lipid bilayers near the phase transition, in: E.A. Disalvo, S.A. Simon (Eds.), *Permeability and Stability of Lipid Bilayers*, CRC Press, Boca Raton, 1995, pp. 137–160.
- [25] J.F. Nagle, H.L. Scott, Lateral compressibility of lipid mono- and bilayers. Theory of membrane permeability, *Biochim. Biophys. Acta* 513 (1978) 236–243.
- [26] E. Evans, R. Kwok, Mechanical calorimetry of large dimyristoylphosphatidylcholine vesicles in the phase transition region, *Biochemistry* 21 (1982) 4874–4879.
- [27] M. Bloom, E. Evans, O.G. Mouritsen, Physical properties of the fluid lipid-bilayer component of cell membranes: a perspective, *Q. Rev. Biophys.* 24 (1991) 293–397.
- [28] J.A.F. Op den Kamp, Lipid phase transition of phosphatidylglycerol in acholeplasma laidlawii membranes studied with phospholipase A<sub>2</sub>, *Rev. Infect. Dis.* 4 (1982) 80–84.
- [29] M. Menashe, G. Romero, R.L. Biltonen, D. Lichtenberg, Hydrolysis of dipalmitoylphosphatidylcholine small unilamellar vesicles by porcine pancreatic phospholipase A<sub>2</sub>, *J. Biol. Chem.* 261 (1986) 5334–5340.
- [30] T. Hønger, K. Jørgensen, R.L. Biltonen, O.G. Mouritsen, Systematic relationship between phospholipase A<sub>2</sub> activity and dynamic lipid bilayer microheterogeneity, *Biochemistry* 35 (1996) 9003–9006.
- [31] A.J. Metso, A. Jutila, J.-P. Mattila, J.M. Holopainen, P.K.J. Kinnunen, Nature of the main transition of dipalmitoylphosphocholine bilayers inferred from fluorescence spectroscopy, *J. Phys. Chem., B* 107 (2003) 1251–1257.
- [32] A.J. Metso, J.-P. Mattila, P.K.J. Kinnunen, Characterization of the main transition of dinervonoylphosphocholine liposomes by fluorescence spectroscopy, *Biochim. Biophys. Acta* 1663 (2004) 222–231.
- [33] T. Heimburg, A model for the lipid pretransition: coupling of ripple formation with the chain-melting transition, *Biophys. J.* 78 (2000) 1154–1165.
- [34] D.P. Kharakoz, E.A. Shlyapnikova, Thermodynamics and kinetics of the early steps of solid-state nucleation in the fluid lipid bilayer, *J. Phys. Chem., B* 104 (2000) 10368–10378.
- [35] J.-M.I. Alakoskela, P.K.J. Kinnunen, Phospholipid main phase transition assessed by fluorescence spectroscopy, in: C.D. Geddes, J.R. Lakowicz (Eds.), *Annu. Rev. Fluorescence*, vol. I, Kluwer Academic/Plenum Publishers, New York, 2004, pp. 257–297.
- [36] A. Jutila, P.K.J. Kinnunen, Novel features of the main transition of dimyristoyl–phosphocholine bilayers revealed by fluorescence spectroscopy, *J. Phys. Chem. B* 101 (1997) 7635–7640.
- [37] A. Chattopadhyay, Chemistry and biology of *N*-(7-nitrobenz-2-oxa-1,3-diazol-4-yl)-labeled lipids: fluorescent probes of biological and model membranes, *Chem. Phys. Lipids* 53 (1990) 1–15.
- [38] R.M. Weis, Fluorescence microscopy of phospholipid monolayer phase transitions, *Chem. Phys. Lipids* 57 (1991) 227–239.
- [39] S.K. Wiedmer, M.S. Jussila, J.M. Holopainen, J.-M. Alakoskela, P.K.J. Kinnunen, M.-L. Riekkola, Cholesterol-containing phosphatidylcholine liposomes: characterization and use as dispersed phase in electrokinetic capillary chromatography, *J. Sep. Sci.* 25 (2002) 427–437.



- [40] P.J. Patty, B.J. Frisken, The pressure-dependence of the size of extruded vesicles, *Biophys. J.* 2 (2003) 996–1004.
- [41] M.I. Angelova, S. Soleau, P.H. Meleard, J.F. Faucon, P. Bothorel, Preparation of giant vesicles by external AC electric fields. Kinetics and applications, *Prog. Colloid & Polym. Sci.* 89 (1992) 127–131.
- [42] T. Brumm, K. Jorgensen, O.G. Mouritsen, T.M. Bayerl, The effect of increasing membrane curvature on the phase transition and mixing behavior of a dimyristoyl-*sn*-glycero-3-phosphocholine/distearoyl-*sn*-glycero-3-phosphocholine lipid mixture as studied by Fourier transform infrared spectroscopy and differential scanning calorimetry, *Biophys. J.* 70 (1996) 1373–1379.
- [43] L.A. Bagatolli, E. Gratton, Two-photon fluorescence microscopy observation of shape changes at the phase transition in phospholipid giant unilamellar vesicles, *Biophys. J.* 77 (1999) 2090–2101.
- [44] D. Needham, E. Evans, Structure and mechanical properties of giant lipid (DMPC) vesicles bilayers from 20 °C below to 10 °C above the liquid crystal-crystalline phase transition at 24 °C, *Biochemistry* 27 (1988) 8261–8269.
- [45] R.S. Brown, J.D. Brennan, U.J. Krull, Self-quenching of nitrobenzoxadiazole labeled phospholipids in lipid membranes, *J. Chem. Phys.* 100 (1994) 6019–6027.
- [46] V. Tsukanova, D.W. Grainger, C. Salesse, Monolayer behavior of NBD-labeled phospholipids at the air/water interface, *Langmuir* 18 (2002) 5539–5550.
- [47] R.F.M. de Almeida, L.M.S. Loura, A. Fedorov, M. Prieto, Non-equilibrium phenomena in the phase separation of a two-component lipid bilayer, *Biophys. J.* 82 (2002) 823–834.
- [48] A. Chattopadhyay, E. London, Parallax method for direct measurement of membrane penetration depth utilizing fluorescence quenching by spin-labeled phospholipids, *Biochemistry* 26 (1987) 39–45.
- [49] F.S. Abrams, E. London, Extension of the parallax analysis of membrane penetration depth to the polar region of model membranes: use of fluorescence quenching by a spin-label attached to the phospholipid polar headgroup, *Biochemistry* 32 (1993) 10826–10831.
- [50] J.M. Sturtevant, The effects of water-soluble solutes on the phase transitions of phospholipids, *Proc. Natl. Acad. Sci. U. S. A.* 81 (1984) 1398–1400.
- [51] J. Lemmich, J.H. Ipsen, T. Hønger, T. Bauer, O.G. Mouritsen, Pseudocritical behavior and unbinding of phospholipid bilayers, *Phys. Rev. Lett.* 75 (1995) 3958–3961.
- [52] P.C. Mason, J.F. Nagle, R.M. Epand, J. Katsaras, Anomalous swelling in phospholipid bilayers is not coupled to the formation of a ripple phase, *Phys. Rev., E* 63 (2001) 030902–030904.
- [53] G.E.S. Toombes, A.C. Finnefrock, M.W. Tate, S.M. Gruner, Determination of L-H<sub>II</sub> phase transition temperature for 1,2-dioleoyl-*sn*-glycero-3 phosphatidylethanolamine, *Biophys. J.* 5 (2002) 2504–2510.
- [54] B. Tenchov, On the reversibility of the phase transitions in lipid–water systems, *Chem. Phys. Lipids* 57 (1991) 165–177.
- [55] B.Z. Chowdhry, G. Lipka, A.W. Dalziel, J.M. Sturtevant, Multi-component phase transitions of diacylphosphatidylethanolamine dispersions, *Biophys. J.* 45 (1984) 901–904.
- [56] M. Rappolt, G. Rapp, Simultaneous small- and wide-angle X-ray diffraction during the main transition of dimyristoyl ethanolamine, *Ber. Bunsenges. Phys. Chem.* 100 (1996) 1153–1162.
- [57] J.H. Ipsen, O.G. Mouritsen, Decoupling of the crystalline and conformational degrees of freedom in lipid monolayers, *J. Chem. Phys.* 91 (1989) 1855–1865.
- [58] K. Jørgensen, Calorimetric detection of a sub-main transition in long-chain phosphatidylcholine lipid bilayers, *Biochim. Biophys. Acta* 1240 (1995) 111–114.
- [59] M. Nielsen, L. Miao, J.H. Ipsen, K. Jorgensen, M.J. Zuckermann, O.G. Mouritsen, Model of a sub-main transition in phospholipid bilayers, *Biochim. Biophys. Acta* 1283 (1996) 170–176.
- [60] M. Caffrey, The study of lipid phase transition kinetics by time-resolved X-ray diffraction, *Annu. Rev. Biophys. Biophys. Chem.* 18 (1989) 159–186.
- [61] B. Tenchov, H. Yao, I. Hatta, Time-resolved X-ray diffraction and calorimetric studies at low scan rates: I. Fully hydrated DPPC and DPPC/water/ethanol phases, *Biophys. J.* 56 (1989) 757–768.
- [62] G. Rapp, M. Rappolt, O. Laggner, Time-resolved simultaneous small- and wide-angle X-ray diffraction on dipalmitoyl–phosphatidylcholine by laser temperature-jump, *Prog. Colloid & Polym. Sci.* 93 (1993) 25–29.